Numerical analysis of p-GaAs/n-GaAs tunnel junction employing InAs intermediate layer for high concentrated photovoltaic applications

Seokjin Kang,[1] Kwang Wook Park,[1] Sooraj Ravindran,[1] and Yong Tak Lee[1*]

[1]School of Information and Informations, Gwangju Institute of Science and Technology (GIST), 123, Cheomdangwagi-ro, Buk-gu, Gwangju 500-712, Republic of Korea

E-mail: ytlee@gist.ac.kr

Abstract. We report the numerical analysis of p-GaAs/n-GaAs tunnel junction employing InAs as the intermediate layer at the junction. Incorporation of this intermediate layer introduces an intermediate level at the junction bandgap leading to enhanced tunneling of carriers. By doing so, we obtain a two order of enhancement in the tunnel current. Furthermore, the performance of GaInP/GaAs dual-junction solar cells using the TJ with InAs intermediate layer is calculated under concentrated suns condition and it shows a conversion efficiency exceeding 30% under 1800 suns condition.

1. Introduction

A tunnel junction (TJ) supplying high current is one of the key requirements to achieve high efficiency in high concentrated photovoltaic (CPV) applications. Recently, multi-junction solar cells using $Ga_{0.51}In_{0.49}P$ (1.9 eV band gap), GaAs (1.43 eV band gap) and $Ga_{0.69}In_{0.31}As$ (1.0 eV band gap) have been reported having a conversion efficiency of 44.4% at 302 suns [1]. To operate the solar cells under high concentrated sun (>1000 suns) condition, the TJ that interconnects the sub-cells must provide efficient current transport with small voltage loss by generating high tunnel current [2, 3]. Several methods have been reported to accomplish an increase in the tunnel current, and one such method is by introducing ErAs recombination centers as an intermediate level between the junction interface [4, 5]. It halves the current path length and thus increases the tunnel current drastically. This is because the tunneling probability is related to the inverse exponential of the path length. With the presence of an intermediate level in the junction, peak tunnel current density (I_{peak}) increases by the factor of 2. However, ErAs has a rock-salt crystal structure which is quite dissimilar to the crystal structure of conventional semiconductors used in realizing multi-junction solar cells. This dissimilar crystal structure degrades the device performance due to the introduction of high density of Ga-antisite defects originating from the interface between zinc blende and rock salt structure. As an alternative, InAs (0.35 eV band gap) which has a zinc blende crystal structure similar to that of semiconductor materials used in III-V solar cells can possibly introduce intermediate level at the junction interface by utilizing their lower band gap energy as compared with the other alternative TJ materials such as GaInP, $Al_{0.38}Ga_{0.62}As$ (1.9 eV band gap) and GaAs without introducing serious defects. Experimental demonstration of this concept has already has been reported, which shows two orders of I_{peak} enhancement in GaAs TJ with InAs quantum dot as the intermediate level [6]. However, numerical simulation of TJs employing intermediate level has not been well studied yet. In this paper, we report the numerical analysis of GaAs TJ employing InAs intermediate level and GaInP/GaAs dual-junction solar cells employing the TJ under concentrated suns condition.

2. Theoretical models for numerical simulations

2.1 Carrier statistics model

The carriers in the highly doped degenerate layers in which Fermi level no longer exists in the band gap obey a different statistical behavior as compared with non-degenerate semiconductors which obeys Boltzmann statistics. To operate the p-GaAs/n-GaAs structure as a TJ, the two oppositely doped layers should be highly doped. Furthermore, band gap narrowing effect and Fermi-Dirac statistics must be considered to accurately analyze the behavior carriers in highly doped regions. The band gap narrowing effect is related to doping concentration of the layer, and expressed as

$$\Delta E_g = A\left\{\ln\frac{N}{B} + \left[\left(\ln\frac{N}{B}\right)^2 + 0.5\right]^{\frac{1}{2}}\right\} \quad (1)$$

where constant A and B are $9.0\text{x}10^{-3}$ eV and $1.0\text{x}10^{17}$ cm^{-3}, respectively, obtained from Slotboom [7], and N represents the doping concentration. The amount of bandgap narrowing for a doping concentration of 10^{19} cm^{-3} was about 61 meV. Fermi-Dirac statistics describes the probability that an available electron state with energy E is occupied by an electron and is given by

$$\mathrm{f}(\varepsilon) = \frac{1}{1+exp\left(\frac{\varepsilon - E_F}{kT}\right)} \quad (2)$$

In the limiting case, $\varepsilon - E_F \gg kT$, equation 2 has much simpler form like $\mathrm{f}(\varepsilon) = exp\left(\frac{E_F-\varepsilon}{kT}\right)$ referred to as Boltzmann statistics. However, we used Fermi-Dirac statistics because the limiting case is not applicable for highly doped material.

2.2 Tunneling model

Tunneling at the TJ is basically driven by the real spatial transport of carriers through the barriers. This non-local band-to-band tunneling can be significant for small tunneling path length. Tunnel current density for an electron with longitudinal energy E and transverse energy E_T is given by

$$\mathrm{J}(E) = \frac{q}{\pi\hbar}\iint T(E)\,[f_l(E+E_T) - f_r(E+E_T)]\rho(E_T)dEdE_T \quad (3)$$

where T(E) is the tunneling probability for an electron with longitudinal energy E and $\rho(E_T)$ is the 2D density of states corresponding to the two transverse wavevector components. f_l and f_r represenets the Fermi-Dirac functions on the left and right hand side of the junction.

The tunneling probability is calculated using the WKB approximation and it is given by

$$\mathrm{T}(E) = exp\left(-2\int_{x_{start}}^{x_{end}} k(x)dx\right) \quad (4)$$

where x_{start} and x_{end} are the start and end points of the tunneling paths. The commercial Silvaco Atlas 2D TCAD provides these non-local tunneling band-to-band model and WKB approximation for the tunneling probability and our simulations were performed by using these models [8].

3. Simulation procedure

Prior to analyzing the GaInP/GaAs dual junction solar cell, p-GaAs/n-GaAs TJ structures were analyzed. Two different TJ structures with fine mesh structures were generated (Fig. 1). The reference structure (Fig. 1(a)) was a GaAs tunnel diode with 25 nm-thick p+GaAs and n+GaAs, and the doping concentration of the compositing layers was in the range from 10^{18} cm^{-3} to 10^{20} cm^{-3}. The mesh structure was defined by five separate divisions of 100 um-thicknesses along horizontal direction, and one hundred separate divisions of 50 nm-thicknesses along vertical direction. The direction of the current flow was also along the vertical direction. In addition, two hundred separate divisions of 30 nm-thicknesses along vertical direction near the junction were generated for the accurate calculation of non-local band-to-band tunneling modeling. For the second structure (Fig. 1(b)), InAs intermediate layer was inserted at the junction interface of the reference TJ. The same mesh structure was employed for the calculation since the number of meshes can possibly affect the accuracy of simulations. By using the above TJ structures, we calculated I-V curve and extracted I_{peak} and peak voltage (V_{peak}) which are shown in Fig. 1(c). First, the doping concentrations of p-GaAs and n-GaAs region of the reference TJ and TJ with InAs intermediate level was varied to compare their performance, and the resulting I_{peak} contour plots were generated. Second, the doping concentration, doping type and thickness of InAs intermediate layer was varied to find out the effect of these parameters on the TJ current. During the calculations, the doping concentration of p-GaAs and n-GaAs was fixed at $4\text{x}10^{19}$

cm^{-3} and 10^{19} cm^{-3}. Next, TJ employing InAs intermediate layer was incorporated in the GaInP/GaAs dual-junction solar cell (Fig 2). InAs was n-doped with a carrier concentration of 10^{19} cm^{-3} and the thickness was 3.7 nm. Additionally, current matching between GaInP and GaAs subcells was applied. SiO_2/Si_3N_4 double layer anti-reflection coating (DARC) ensured the reduction of surface reflection and metal shadowing area was assumed to be 5% of whole area. Solar spectrum with an air mass 1.5 global (AM 1.5G) under normal solar incidence was used in simulations. The performance of the solar cell was calculated up to 2000 concentrated suns condition.

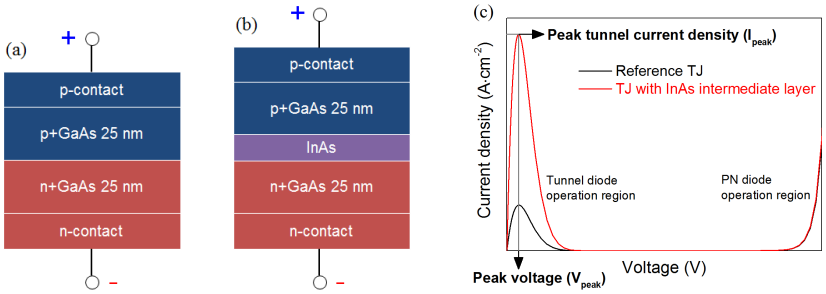

Figure 1 (a) Reference structure (b) TJ with InAs intermediate layer, and (c) I-V curve for the reference structure and TJ structure with InAs intermediate layer

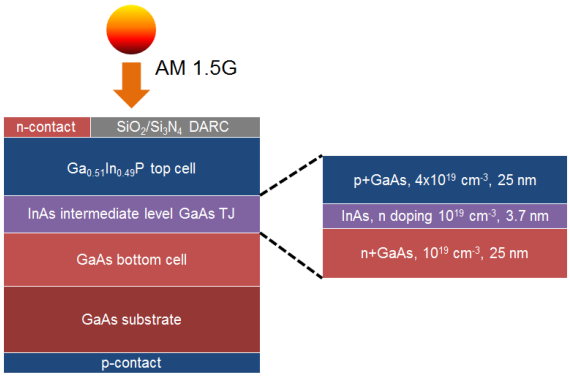

Figure 2 GaInP/GaAs dual-junction solar cell structure

4. Results and discussion

By varying the p and n GaAs doping concentration, the contour plot describing the minimum required doping concentration in order for the solar cell to operate in 100 suns (1.3 $A{\cdot}cm^{-2}$) and 1000 suns (13 $A{\cdot}cm^{-2}$) are illustrated in Fig. 3. It clearly shows that the TJ structure with InAs in the intermediate level requires lower doping concentration than the reference TJ. In addition, for the same doping concentration, a two order enhancement for I_{peak} was obtained in TJ with InAs in the intermediate level compared to that of the conventional one as expected since the tunneling probability is proportional to inverse exponential of the tunneling path. The presence of InAs intermediate level divided the tunneling path length in to half resulting in a large increase of tunnel current. However, at higher doping concentrations (>$5{\times}10^{19}$ cm^{-3}), there was only an order of enhancement since the tunneling path length was already short enough in this condition.

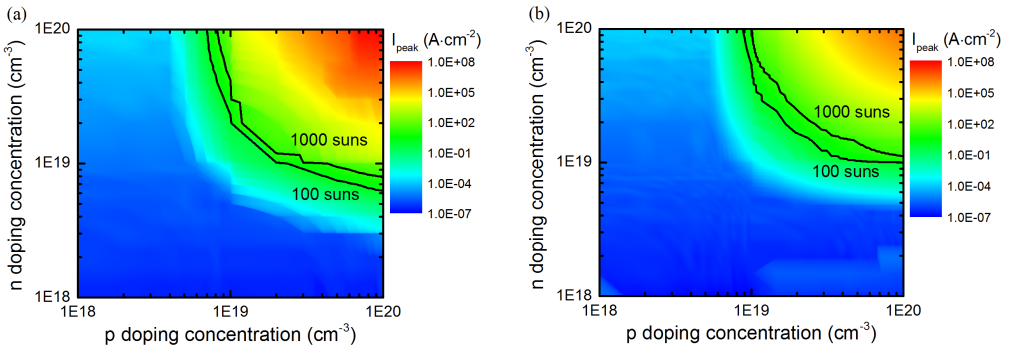

Figure 3 Contour plots of I_{peak} for (a) the reference TJ and (b) TJ with InAs as the intermediate level

Further simulations were done by varying the p and n doping concentration and thickness of InAs layer. It was found that n-type doping for InAs was suitable, while p-type doping was not suitable for enhancing the tunnel current. With the increase of n-type carrier concentration, I_{peak} exponentially increased at ultra-high doping concentration region (Fig. 4). This is because of the band alignment which aids the electron tunneling. In the GaAs/InAs system, conduction band offset is 0.69 eV and valence band offset is 0.38 eV [9]. Since the conduction band offset is larger than valence band offset, using the intermediate level at the conduction band (Fig. 5(b)) provides shorter tunneling path length than the case when intermediate level is used at the valence band (Fig 5(a)). However, V_{peak} was similar regardless of the change in doping concentration because it largely depends on the doping concentration of p and n GaAs regions rather than that of InAs region. For varying InAs thickness, it was found that I_{peak} increased continuously (Fig. 6(a)). This is attributed to the formation of intermediate level, and as a result more carriers could tunnel across the p+GaAs and n+GaAs sides compared to the case when intermediate level was absent. Thus, as the InAs thickness was increased, the tunnel current also increased.

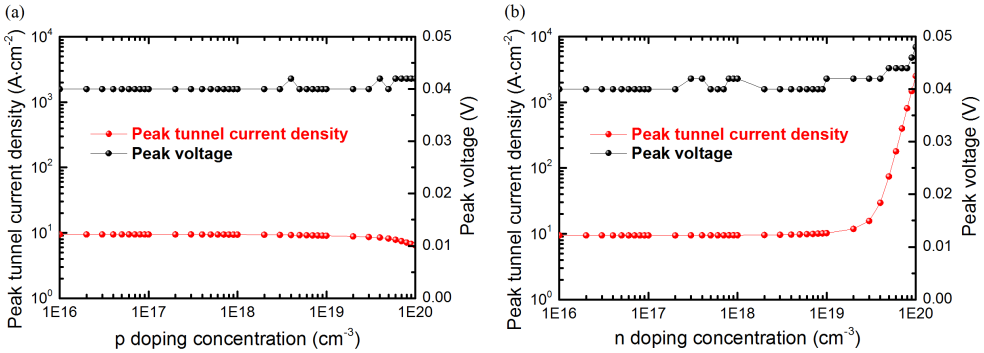

Figure 4 Variation of tunnel current as a function of (a) p doping and (b) n doping of InAs

It was also found that GaInP/GaAs dual-junction solar cells with TJs employing InAs intermediate level operated well up to 2000 suns condition. The conversion efficiency was over 30% up to 1800 suns and there was no significant degradation in efficiency caused by absorption at the InAs layer (Fig. 6(b)). This was because the thickness of InAs was small enough to cause any appreciable optical loss. Incorporation of InAs intermediate level provided about 400 times larger I_{peak} than normal GaAs TJ and it could also enable the operation of solar cell under high concentration suns. For a normal GaAs TJ, the solar cell could only operate up to a low concentration of 10 suns.

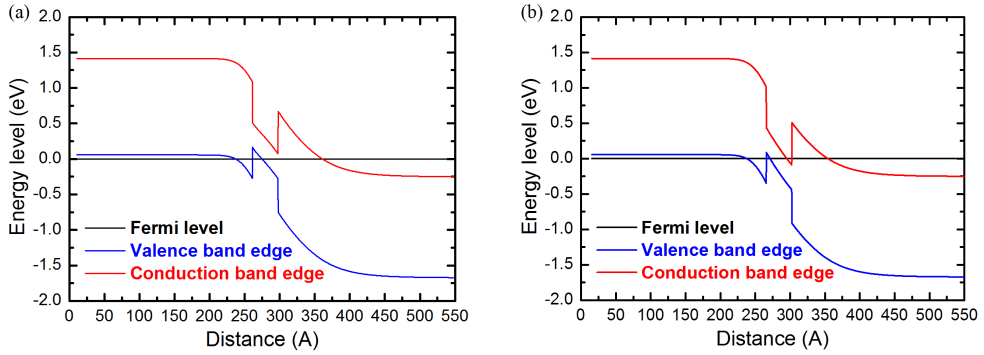

Figure 5 Band diagrams of p-GaAs/n-GaAs TJ with InAs intermediate layer. (a) shows the case when InAs is p doped and (b) denotes the case when InAs is n doped.

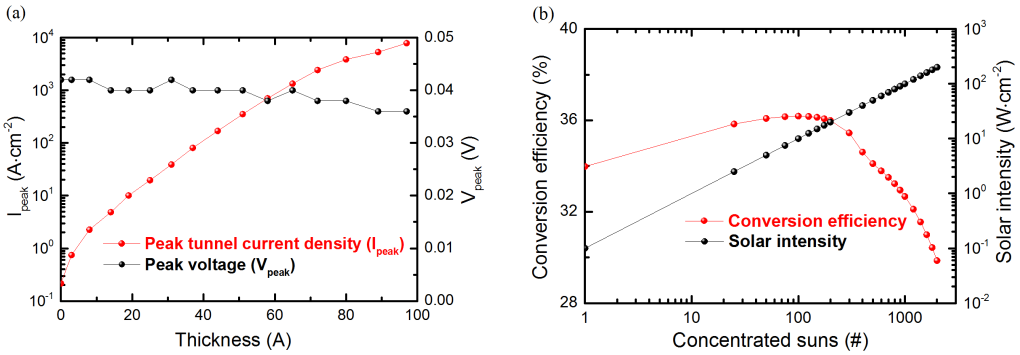

Figure 6 (a) I_{peak} and V_{peak} of GaAs TJ with InAs intermediate layer for various interlayer thickness and (b) performance of GaInP/GaAs dual-junction solar cells using InAs intermediate level

5. Conclusion

The performance of GaAs TJ with InAs embedded as the interlayer at the junction was evaluated using Silvaco 2D TCAD. It was found that TJ with InAs incorporated at the junction introduced an intermediate level in the bandgap resulting in about two order of increment in I_{peak}. We investigated about the type of doping suitable for the InAs interlayer, and found that n-type doping was the appropriate one. With increasing thickness of InAs layer, I_{peak} also increased, which was due to the increase in tunneling by the presence of intermediate layer. In addition, we also studied the performance of GaInP/GaAs dual-junction solar cells employing InAs as the intermediate level, and found that it operated up to 2000 suns condition and maintained energy conversion efficiency nearly 30%, while without InAs interlayer, the operation was limited only to low concentration of 10 suns. It could be expected that incorporating interlayer to various TJs of solar cells could result in improved performance of concentrated photovoltaics.

AKNOWLEDGEMENT

This work was supported by the National Research Foundation of Korea (NRF) grant funded by the Korea government (MEST) (No. 2011-0017606).

References

[1] M. A. Green, K. Emery, Y. Hishikawa, W. Warta and E. D. Dunlop 2013 *Prog. Photovolt: Res. Appl.* **21** 827-837.
[2] R. R. King, D. C. Law, K. M. Edmondson, C. M. Fetzer, G. S. Kinsey, H. Yoon, R. A. Sherif, and N. H. Karam 2007 *Appl. Phys. Lett.* **90** 183516.
[3] R. R. King, R. A. Sherif, D. C. Law, J. T. Yen, M. Haddad, C. M. Fetzer, K. M. Edmondson, G. S. Kinsey, H. Yoon, M Joshi, S. Mesropian, H. L. Cotal, D. D. Krut, J. H. Ermer, and N. H. Karam presented at 2006 *21st European Photovoltaic Solar Energy Conference*
[4] Hari P. Nair, Adam M. Crook, and Seth R. Ban 2010 *Appl. Phys. Lett.* **96** 222104
[5] S. Preu, S. Malzer, G. H. Dohler, H. Lu, A. C. Gossard, and L. J. Wang 2010 *Semicond. Sci. Technol.* **25** 115004
[6] L. Wang, J. He, X. Shang, M. Li, Y. Yu, G. Zha, H. Ni, and Z. Niu 2012 *Semicond. Sci. Technol* **27** 115010
[7] Slotboom, J. W. and H. C. De Graaf, 1976 *Solid State Electron.* **19**, 857-862
[8] Silvaco 2D TCAD *Atlas User's Manual* Chapter 3 Physics
[9] R. Colombelli, V. Piazza, A. Badolato, M. Lazzarino, F. Beltram 2000 *Appl. Phys. Lett.* **76** 1146